Cement Kiln Dusts and Their Hydration Products- A Characterization Study

J. Olek, S. Peethamparan
Purdue University, West Lafayette, USA

Abstract

This paper presents the results of a characterization study to evaluate the influence of the chemical and physical properties of four different types of cement kiln dusts (CKDs) on their hydration products. A detailed data on chemical (X-ray diffraction (XRD)) and morphological analysis (scanning electron microscope (SEM)) of both the unhydrated CKD powders and the hydrated CKD samples are presented. In general, it was observed that CKDs with high (~14-29%) content of free-lime upon hydration produced significant amounts of calcium hydroxide, ettringite and syngenite. These CKDs also developed higher unconfined compressive strength compared to CKDs with lower amounts of free-lime.

1. Introduction

Cement kiln dusts (CKDs) are by-product materials generated during the cement manufacturing processes. Similar to what has been observed with other by-products, a desire to minimize the environmental impact of CKDs disposal generates a strong interest in finding an alternative ways for their utilization. However, in order to select the most effective CKDs utilization method, an in-depth understanding of their interaction with other materials and components present in a particular application system is desired. That interaction will largely depend on the chemical and physical characteristics of the CKDs themselves.

In general, the size of the CKDs particles is similar to that of portland cement. Their chemical composition also resembles that of cement and includes alumina, silica, calcium oxide, alkalis and sulfates. However, the amounts of alkalis (Na_2O and K_2O) and sulfates (SO_3) are substantially higher in CKDs compared to cement. Some of the applications that take advantage of these physical and chemical attributes of CKDs include waste solidification [1, 2], portland cement concrete production and block manufacturing [3-7], and construction of hydraulic barriers in landfills [8]. Other reported usages include applications as agricultural fertilizers [9], flowable fill materials [10, 11], mineral fillers in asphalt pavements, fillers in mine reclamation projects, and sorbent materials to remove sulfur dioxide from cement kiln flue gases [12].

Recent studies [12-15] have shown that CKDs can also be used in soil stabilization applications as potential substitute for hydrated lime ($Ca(OH)_2$). Hydrated lime is commonly used as soil stabilizer due to is ability to react with clays (pozzolanic reaction), thus increasing soil's stability [16-17]. Since some CKDs contain considerable amounts of free-lime, a similar stabilization mechanism might be expected to develop in CKD-treated soils. Being relatively complex chemically, when reacting with water, CKDs may produce (in addition to $Ca(OH)_2$) other hydration products that may significantly affect their soil stabilization potential. In addition to the free-lime, the alkalis and sulfates present in the CKDs may also play a significant role in the hydration process.

The objective of the present study was to characterize several different CKDs and to evaluate the influence of their chemical and physical properties on the hydration products. The characterization study included the physical analysis of CKD powders (particle size distribution and specific surface area), the chemical analysis (X-ray fluorescents spectroscopy (XRF), XRD) and morphological analysis (SEM) of both CKD powders and the hydrated CKD samples. In addition, in an attempt to correlate the physical and chemical properties of CKDs with their performance, the unconfined compressive strength of compacted CKDs (as a relative measure of their reactivity) was also determined.

2. Material Selection

Four CKDs (from now on referred to as CKD-1, CKD-2, CKD-3 and CKD-4) were selected, each from a different cement plant, for the present study. The chemical composition of these CKDs was determined by XRF spectroscopy, and is presented in Table 1. For comparative purposes, chemical composition of a typical Type I portland cement is also included in this table. Similar to Type I portland cement, the CKDs contain significant amounts of calcium oxide (CaO), silicon dioxide (SiO_2), alumina (Al_2O_3) and ferrous oxide (Fe_2O_3). However, the sulfur trioxide (SO_3) and alkali (K_2O and Na_2O) contents, which are strictly controlled in ordinary portland cement, were significantly higher in the CKDs. The unreacted CaO (or free-lime), which is expected to play a major role in the soil stabilization, was highest (29.14%) in CKD-2, followed by CKD-1 (13.85%). The free-lime content in the remaining two CKDs was relatively low (5.32% in CKD-3 and 3.26% in CKD-4).

The particle size distributions of these CKDs, determined using a laser particle size analyzer, are shown in Fig. 1. From the particle size distribution measurements the surface area values were calculated. For comparative purposes, the particle size distribution of a typical Type I portland cement is also shown in Fig.1. CKD-1 had the finest particles with an average particle size of 8 μm and the surface area of 0.41 m^2/g.

CKD-2, on the other hand, had the coarsest particles with an average particle size of 30 μm and calculated surface area of 0.30 m^2/g. CKD-3 and CKD-4 had particle size distributions very similar to that of the Type I portland cement, with an average particle size of approximately 15 μm and the surface areas, respectively, of 0.36 m^2/g and 0.34 m^2/g.

Table 1 Chemical composition of CKDs

	CKD-1	CKD-2	CKD-3	CKD-4	Type I Cement
Chemical composition by XRF	Weight (%)				
SiO_2	12.18	16.42	11.91	15.39	20.48
Al_2O_3	4.24	3.62	2.17	4.66	4.21
TiO_2	0.22	0.23	0.15	0.57	0.36
P_2O_5	0.08	0.09	0.09	0.09	0.09
Fe_2O_3	1.71	2.31	2.08	2.34	2.41
CaO	46.24	55.00	46.05	37.35	63.19
MgO	1.24	2.68	2.2	2.10	4
Na_2O	0.51	0.17	0.33	0.81	0.19
K_2O	4.89	2.89	1.43	7.0	0.28
Na_2O equiv.	3.72	2.05	1.27	5.36	
Mn_2O_3	0.05	0.44	0.04	0.07	0.14
SrO	0.04	0.03	0.07	0.02	0.04
SO_3	14.62	12.69	4.21	5.80	2.76
Cl	0.59	0.74	0.35	3.26	-
LOI@ 750	14.22	3.92	29.63	27.65	1.76
free CaO **	13.85	29.14	5.32	3.26	1.58

**Determined using the chemical analysis

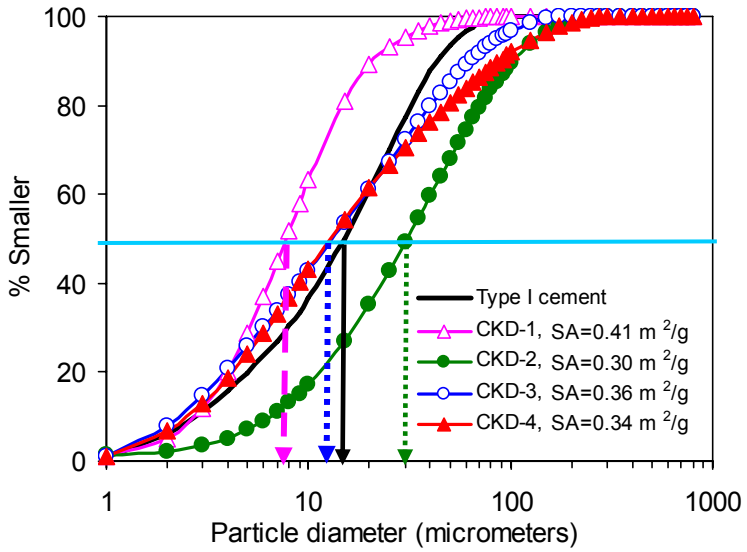

Fig. 1. Particle size distribution of the CKD powders

3. Experimental Program and Sample Preparations

The chemical compositions of the CKDs presented in the previous section (Table 1) were determined by XRF spectroscopy and were supplied by the cement company. Additional measurements, such as XRD, SEM and energy dispersive X-ray spectrometry (EDX) were carried as a part of this study and are briefly described in the following sections.

3.1 X-ray diffraction (XRD) analysis

The XRD analysis was carried out using Siemens D-500 diffractometer with CuKα as a radiation source and a tube powered to 50 kV and 30 mA. The random powder mount specimens were scanned from 3 to 65^{o} 2θ at 0.02^{o} sep size. The hydrated samples were obtained from small cylinders, which were produced by mixing each of the CKDs with 31% of water (by weight) and compacting the resulting paste in a steel mold. The cylinders were extracted from the molds immediately after compaction, and were then wrapped in plastic bags which were placed in a sealed plastic box. The box was stored in 100% relative humidity room kept at constant temperature of 23^{o}C. After the predetermined curing periods (1, 7 and 28 days), small size (1x1x1 cm) cubical samples were cut from the cylinders, soaked in acetone for two days to stop hydration, and dried in air for 2 days. The powder samples were prepared by grinding a part of the small cubical samples and sieving them through a 200 mesh (75 μm) sieve. These samples were used to prepare the randomly-oriented powder mount X-ray specimens. Interpretation of the X-ray patterns was carried out by usual methods, involving assignment of each of the peaks visible in the pattern to one (sometimes more than one) of the probable crystalline phases.

3.2 Scanning electron microscopy (SEM)

The morphologies of the CKD powders and their hydration products were examined using SEM. The particulate samples (CKD powders as received from the plant) were sprinkled onto double sided Scotch tape®. The small size cubic specimens prepared as described earlier (in section 3.1) were split-opened to reveal a clean fracture surface and mounted on aluminum stubs using carbon tape and silver paint. The samples were coated with platinum. They were then imaged in the secondary mode followed by EDX analysis. Imaging was performed with the FEI NOVA nanoSEM field emission scanning electron microscope using the ET (Everhart-Thornley) or TLD (Through-the-Lens Detector) detectors. The EDX was performed using an Oxford INCA 250 system.

3.3 Unconfined compressive strength (UCS)

The UCS test specimens were prepared at constant amount of water (31% by weight) and compacted in the Harvard miniature compaction apparatus following the procedures described in the USBR-5510 [18] standard. The weight of the compacting hammer was 18.14 kg (40 lb) and 20 blows per layer were applied. Immediately after compaction, the samples were sealed in plastic bags and stored in a watertight plastic box, placed in a 100% relative humidity room kept at constant temperature (23°C). The unconfined compressive strength was determined after 1, 7, 28 and 90 days of curing. Three replicate samples were tested at each age, following procedures described in ASTM D 2166 [19]. The average of the three values was used in the analysis. The compressive strength test was performed using the displacement controlled universal testing machine operated at a strain rate of 1% per minute.

4. Results and Discussion

4.1 X-ray analysis

The oxides present in the CKDs may exist in various mineralogical phases, each with different reactivity. The mineral phases present in the CKD's were determined from XRD patterns, which are shown in Fig. 2.

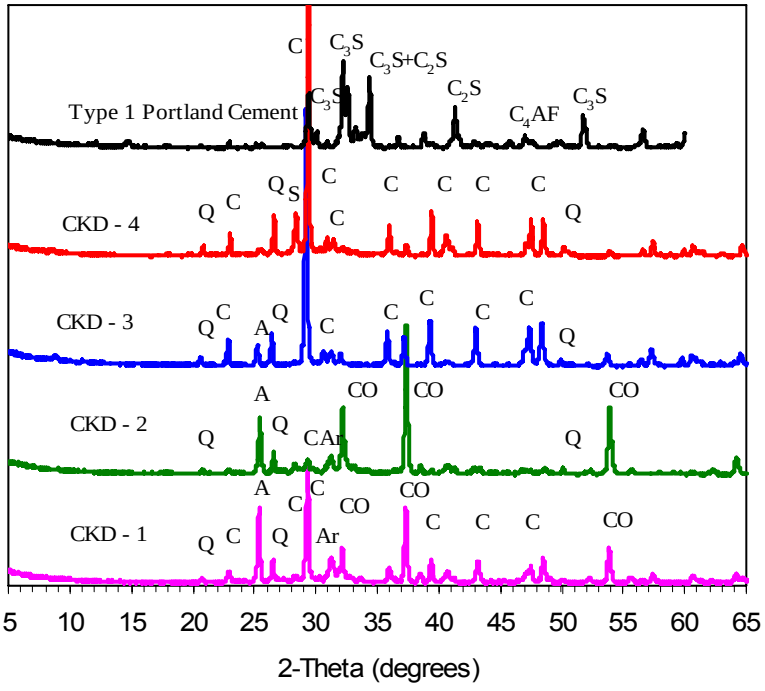

Fig. 2. XRD patterns of CKD powders (Q-quartz, A-anhydrite, C-calcite, S-sylvite, CO-free-lime (calcium oxide), Ar-arcanite).

In all four CKDs considered in this study, the analytical CaO actually existed in three different compounds - $CaCO_3$ (calcite), $CaSO_4$ (anhydrite), and free CaO (free-lime). The strongest free-lime peaks were observed in CKD-2 and CKD-1 materials, respectively, with only very weak peaks present in CKD-3 and CKD-4 patterns. The relative strength of the peaks corresponded well with chemical information reported in Table 1. The calcite content was low in CKD-2, but relatively strong peaks were visible for CKD-3 and CKD-4 materials. Peaks for quartz (SiO_2), arcanite (K_2SO_4) and sylvite (KCl) phases were also identified

The type and the amount of products formed when CKDs react with water will play a major role in determining their effectiveness as potential soil stabilizers. Fig. 3 shows the XRD patterns obtained for the hydrated CKDs after 1, 7, and 28 days of curing.

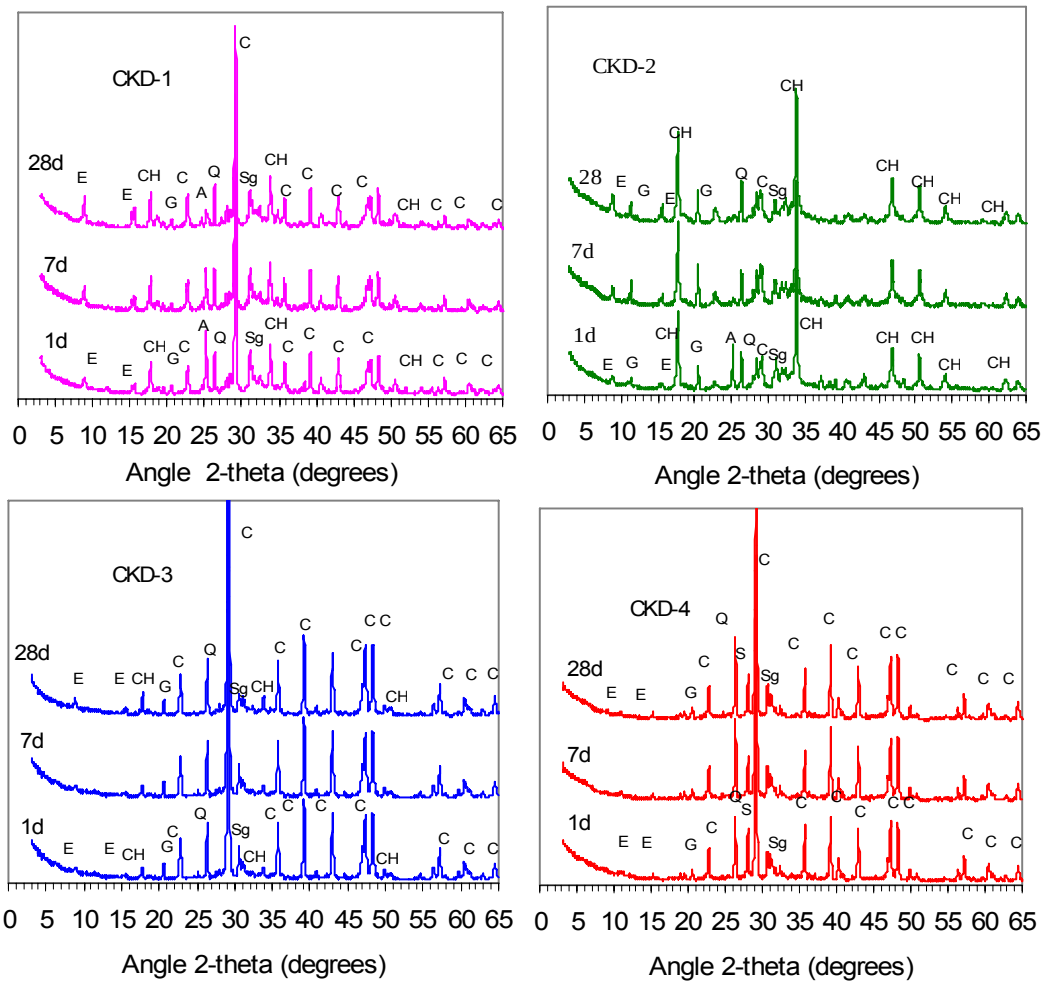

Fig. 3. X-ray patterns of hydrated CKDs hydrated for 1, 7, and 28 days (E-ettringite, CH-calcium hydroxide, G-gypsum, A-anhydrite, Q-quartz, C-calcite, S-sylvite (KCl), Sg-syngenite).

Hydration products of both high free-lime content CKDs (CKD-1 and CKD-2), contained significant amounts of calcium hydroxide (CH), ettringite (E) and syngenite (Sg). In addition to these phases, significant amount of gypsum was found in hydrated CKD-2 while only traces of gypsum were found in CKD-1. The amount of gypsum in CKD-2 increased with an increase in the length of the curing period. In both of these CKDs, the one day cured samples retained some of the anhydrite present in the powder sample. However, the amount of anhydrite gradually decreased with increased curing period, and most of it disappeared by 28 days. It appears that upon adding water, the anhydrite present in the powder samples was first converted to gypsum (G). Subsequently, part of the gypsum was used to form either ettringite or syngenite, with the rest of gypsum remaining in an unaltered form. It also appears that all free-lime present in these CKDs was converted to CH shortly after adding water, and that the amount of CH remained almost the same irrespective of the curing period. The crystalline alkali sulfates phases, such as arcanites (K_2SO_4) originally present in dry samples of CKD-1 and CKD-2 materials were not retained in the wet-cured products, indicating their high solubility.

In the hydrated CKDs with low free-lime content (CKD-3 and CKD-4), only relatively small amounts of ettringite and calcium hydroxide were formed. The heights of the XRD peaks for these compounds did not change significantly with the curing period. The height of the XRD peak for the sylvite (KCl) compound found in dry CKD-4 decreased due to the addition of water and further curing.

The calcite and quartz peaks present in all dry CKDs were retained (in the unchanged form) in hydrated CKDs, indicating the inert nature of these two compounds.

4.2 Morphology of CKD powders by scanning electron microscopy

The SEM micrographs of dry CKD powders are shown Fig. 4. In general, most of the CKD particles appear to form agglomerates with poorly defined shapes and only occasional presence of spherical grains can be observed. Large number of very fine deposits covered the surfaces of some of the spherical particles, while other particles retained very smooth surface texture. These spherical particles were probably flyash particles. The EDX spectrum collected from such particles included peaks for Al, Si, K, O and S. The EDX analyses also revealed the presence of calcite, quartz and anhydrite in all CKDs. Fig. 4 also gives an indication of the relative particle sizes in the agglomerates of each CKD.

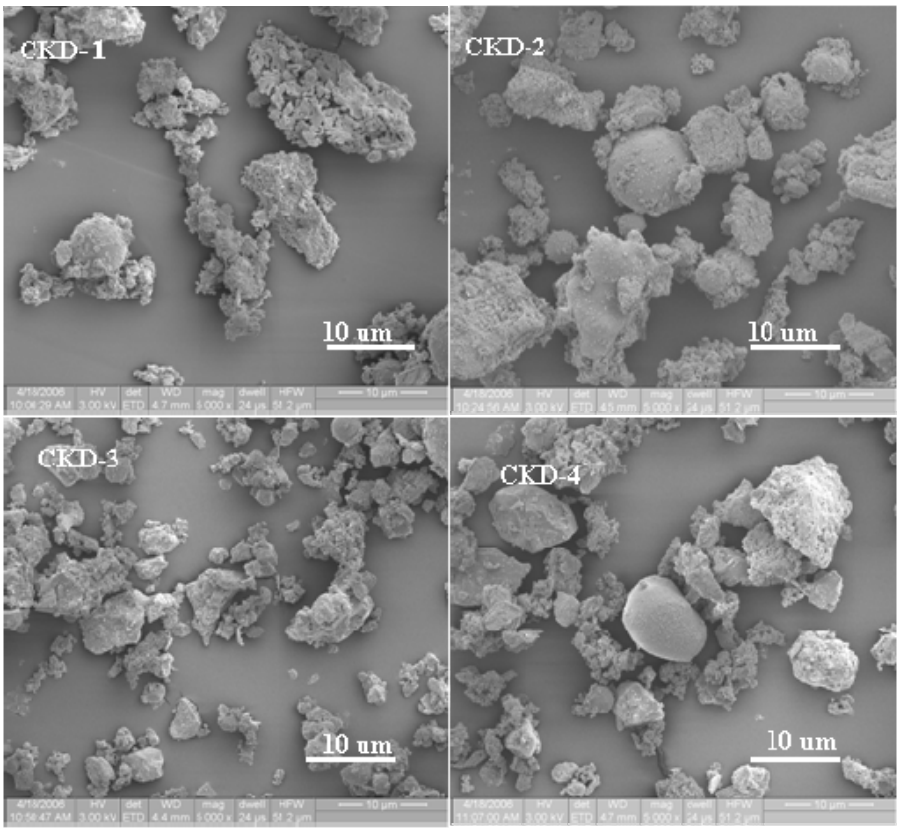

Fig. 4. SEM micrographs of dry CKD powders

Fig. 5(a) shows representative SEM micrographs of CKDs after a hydration period of 28 days. It can be seen that particles' morphology was substantially altered from that of the unhydrated CKDs (Fig. 4). All the spherical particles originally present in the CKD powder disappeared, and new products were formed. One of the prominent features of hydrated CKD-1 and CKD-2 materials was the presence of orthorhombic, lath-shaped particles. These particles were identified by EDX analysis as syngenite ($K_2.Ca(SO_4)_2.2H_2O$), and are marked as "Sg" on the micrographs. The syngenite particles were present in various sizes, and had a smooth surface texture. The other features identified in these two CKDs were hexagonal CH crystals (not shown in the micrograph presented), fine long ettringite needles, and C-S-H-like phases incorporating sulfur in the structure.

On the other hand, the microstructure of hydrated CKD-3 and CKD-4 did not contain lath-shaped syngenite particles. In addition, only few ettringite needles were observed in these CKDs compared to high free-lime content CKDs. The EDX spectrum collected from the C-S-H gel-like structure found in hydrated CKD-3 is shown in Fig. 5(b). Similar spectra were also found in some locations of specimens from the other three CKDs. However, the C-S-H gel-like morphology found in CKD-3 was entirely

different from the morphology of the same material in other CKDs, despite similarity of the EDX's spectra. In the case of CKD-4, the microstructure was dominated by flower petal-like crystals of KCl. Agglomerated particles with peaks for Ca, Si, S and K were also present in CKD-4.

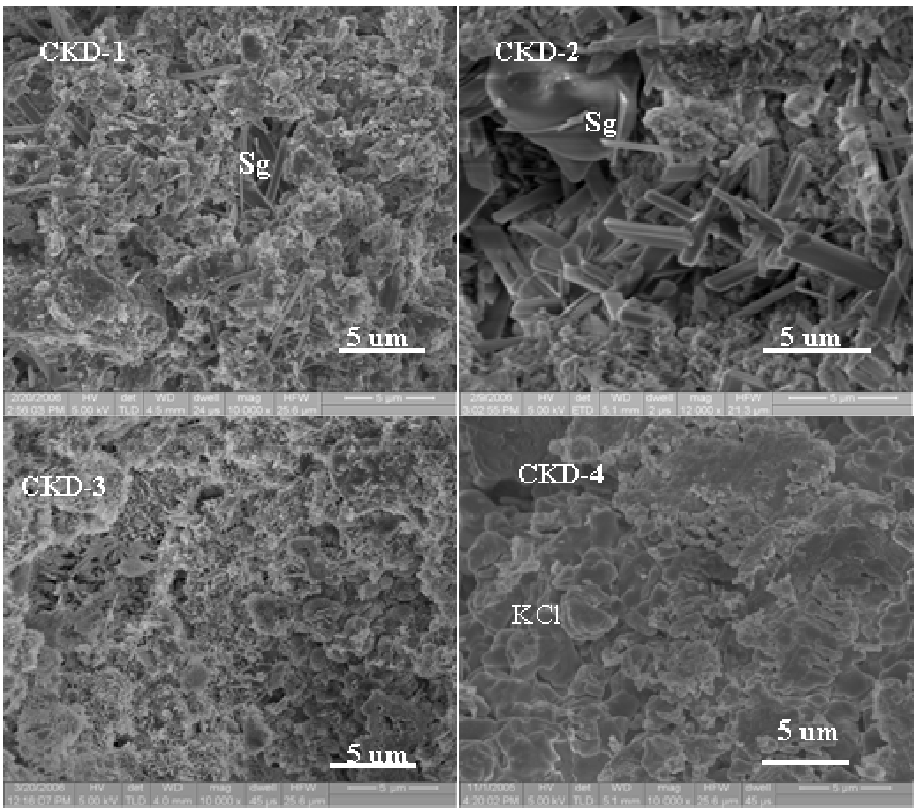

Fig. 5(a). SEM micrographs of hydrated CKDs (28 days old)

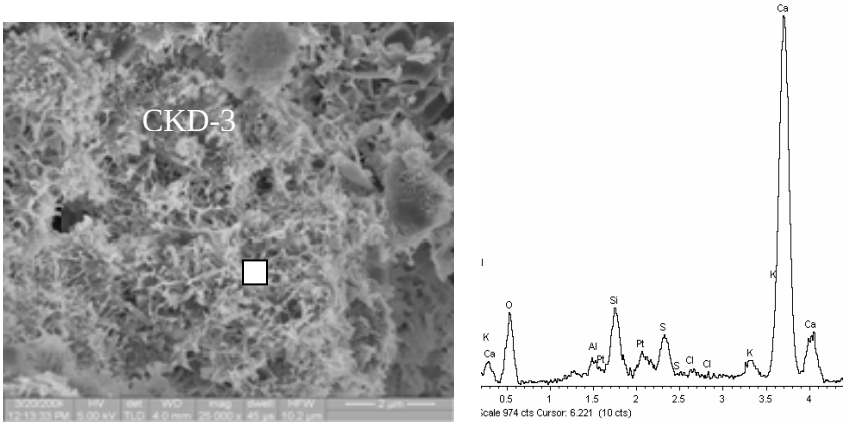

Fig. 5(b). C-S-H-like structure in CKD-3 and EDX spectrum obtained from the given location

4.3 Unconfined compressive strength (UCS)

Strength development is an important parameter that may be used to evaluate the performance of CKDs as potential soil stabilizers. The development of unconfined compressive strength of the CKDs with time is shown in Fig. 6. The high free-lime content CKDs (CKD-1 and CKD-2), achieved significantly higher strength compared to that of the low free-lime content CKDs (CKD-3 and CKD-4). In spite of the significant differences in the free-lime contents of CKD-1 (~14%) and CKD-2 (29%), both of them exhibited similar strength development with time (up to 28 days of curing). This can be attributed to the higher fineness of CKD-1 compared to the fineness of CKD-2. However, for longer curing periods, CKD-2 achieved significantly higher strength compared to that of CKD-1.

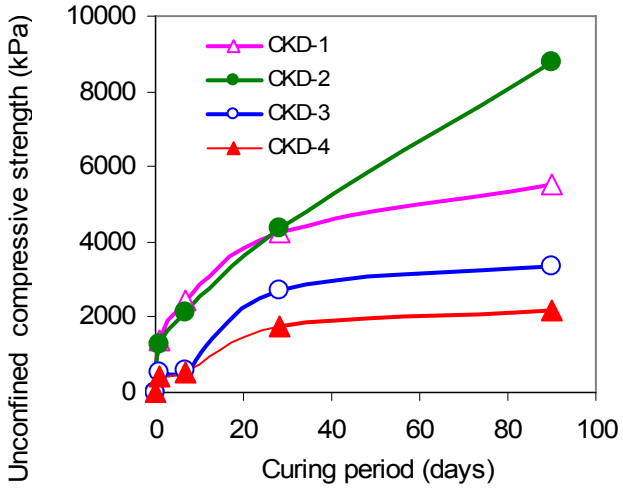

Fig. 6. UCS of the compacted CKD samples

5. Summary

In summary, the high free-lime content CKDs showed better performance in terms of strength development. The XRD, SEM and EDX analysis of hydration products of these CKDs showed presence of C-S-H, CH, ettringite, syngenite and gypsum. The formation of C-S-H by reaction of CH and silica present in the CKDs might have contributed the most towards the strength development. The amounts of reactive SiO_2 present in these CKDs were not determined in this study. However, it is apparent that these CKDs contained some dehydroxilated clays, which is a good source of reactive silica. Though the formation of C-S-H by reaction of CH and SiO_2 is commonly regarded as slow, the presence of large amounts of alkalis in the CKD might have accelerated the pozzolanic reaction [20]. Considerable amounts of other hydration products, such as ettringite, syngenite and gypsum, might have also contributed to strength in the case

of high free-lime content CKDs. The amounts of these products were significantly smaller in the low free-lime content CKDs, and hence resulted in relatively lower strength levels.

6. Conclusions

With the objective of understanding the influence of physical and chemical properties of CKDs on their hydration behavior, a detailed characterization study of four different types of CKDs was conducted. The important conclusions of the present study are:

- Presence of C-S-H, calcium hydroxide, syngenite and ettringite phases were identified in hydrated high free-lime content CKDs. These phases were either absent (or present only in much smaller quantities) in hydrated low free-lime content CKDs
- Hydration process significantly altered the morphology of all CKDs
- Hydrated high free-lime content CKD paste exhibited higher strength compared to that of the low free-lime content CKD pastes at all curing periods.

Acknowledgement

The authors would like to thank Prof. Sidney Diamond of Purdue University and Dr. Laurent Barcelo and Mr. Oscar Tavares of Lafarge North America, for helpful discussions. Ms. Janet Lovell and Mr. Mark Baker are thanked for their support in the Charles Pankow Civil Engineering Materials Laboratory at Purdue University. In addition, the authors would like to acknowledge Lafarge North America for providing the samples of CKDs and for determining their chemical composition.

Reference:

[1] G. A. Miller, S. Azad, Influence of soil type on stabilization with cement kiln dust, Construction and Building Materials 14 (2) (2000) 89-97
[2] M. C. Santagata, A. Bobet, The Use of Cement Kiln Dust (CKD) for Subgrade Stabilization/Modification, SPR 2575, Purdue University, West Lafayette, Indiana, USA, 2002
[3] S. Peethamparan J. Olek, K. Helfrich, Engineering properties of cement kiln dust modified kaolinite clay, 21st International Conference on Solid Waste Technology and Management, Widener University, Philadelphia, March 25-26, 2006, 997-1006.
[4] J. R. Connor, S. Cotton, P.P. Lear, Chemical stabilization of contaminated soils and sludges using cement and cement by products, Proceedings of the Cement Industry Solutions to Waste Management, Calgary, Alberta, Canada, Oct. 7-9, 1992, 73-97

[5] M. MacDay, J. Emery, Stabilization/solidification of contaminated soils and sludges using cementitious systems, Proceedings of the Cement Industry Solutions to Waste Management, Calgary, Alberta, Canada, Oct. 7-9, 1992, 135-151.
[6] M. S. Y. Bhatty, Properties of blended cement made with portland cement, cement kiln dust, fly ash and slag, Proceedings of the 8th International Congress on the Chemistry of Cement, Rio de Janeiro, Brazil, 1986, 118-27
[7] M. L. Wang, V. Ramakrishnan, Evaluation of Blended Cement, Mortar and Concrete made from Type III Cement and Kiln Dust, Construction and Building Materials 4 (2) (1990) 78-97
[8] R. J. Detwile, Bhatty, S. Bhattacharja, Supplementary Cementitious Materials for Use in Blended Cements, R&D Bulletin, RD112, Skokie, Illinois, Portland Cement Association, 1996.
[9] F. F. Udoeyo, A. Hyee, Strength of Cement Kiln Dust Concrete, ASCE Journal of materials in civil engineering Nov./Dec. (2002) 524-526.
[10] G. J. Hawkins, J. I. Bhatty, A. T. O'Hare, Cement kiln dust production, management and disposal, R & D Serial No.2327, Skokie, Illinois, USA: Portland Cement Association, 2003
[11] G. Ballivy, J. Rouis, D. Breton, Use of cement residual kiln dust as landfill liner, Proceedings of the Cement Industry Solutions to Waste Management, Calgary, Alberta, Canada, Oct. 7-9, 1992, 99-118
[12] M. L. Preston, Use of cement kiln dust as an agricultural lime and fertilizer, Presented at the PCA Emerging Technologies Symposium on Cement and Concrete in the Global Environment, Chicago, March 10-11, 1993, in PCA's Cement Technical Support Library DVD020.01©2005
[13] C. E. Pierce, H. Tripathi, T. W. Brown, Cement Kiln Dust in Controlled Low-Strength Materials, ACI Materials Journal 100 (6) (2003) 455-462
[14] A. Katz, K. Kovler, Utilization of Industrial by Product for the Production of Controlled Low Strength Materials (CLSM), Waste Management 24 (2004) 501-512
[15] J. I. Bhatty, Alternative Uses of Cement Kiln Dust, R&D RP 327, Skokie, Illinoise, U.S.A, Portland Cement Association, 1995
[16] S. Diamond, E. B. Kinter, Mechanism of soil-lime stabilization, An Interpretive Review, Highway Research Record (92) (1965) 83-96
[17] J.R. Prusinski, S. Bhattacharja, Effectiveness of Portland Cement and Lime in Stabilizing Clay Soils, Transportation Research Record 1(1652) (1999) 215-227
[18] USBR-5510, Procedure for Performing Laboratory Compaction of Soils-Harvard Miniature, United States Department of the Interior Bureau of Reclamation: Denver, Colorado, 1989
[19] ASTM D 2166, Standard test methods for unconfined compressive strength of cohesive soils, ASTM Int., West Conshohocken, PA, 2000
[20] K. Wang, A. Mishulovich, S.P. Shah, Activations and properties of cementitious materials made with cement-kiln dust and class F fly ash, Journal of materials in civil engineering, Jan (2007)112-119